DOI: 10.61782/fa.2023.0645

forum acusticum 2023

IN-BAND FULL-DUPLEX UNDERWATER ACOUSTIC COMMUNICATIONS USING CODED OFDM AND SIC

Charalampos C. Tsimenidis
Nottingham Trent University, School of Science and Technology
Department of Engineering, Clifton Lane, Nottingham, NG11 8NS, UK

ABSTRACT

This paper focuses on In-band Full-Duplex (IB-FD) based Underwater Acoustic Communication (UAC) systems utilizing Coded Orthogonal Frequency Division Multiplexing (C-OFDM). Presently, most UAC systems utilize Half-Duplex (HD) operation implying that transmission and reception between underwater devices can occur in only one direction at a time. This doubles the latency and halves the limited acoustic bandwidth available. In contrast to HD, IB-FD based systems utilize sophisticated Self-Interference Cancellation (SIC) methods to achieve simultaneous transmission and reception. In-band refers to the fact that the same carrier frequency and acoustic bandwidth is employed for both transmission and reception. The proposed transceiver utilizes a novel adaptive SIC that forms an analog error derived from an attenuated version of the transmitted signal after the power amplifier and the signal received from the local hydrophone. The error is then digitized and used to optimize the SIC filter coefficients. The SIC enables the operation of a C-OFDM system, whose performance is investigated by utilizing experimental signals acquired during seatrials in the North Sea, UK. Numerical Bit-error Rate (BER) results and Signal to Interference and Noise Ratio (SINR) vs. packet index are presented to demonstrate the performance of the proposed transceiver.

Keywords: *Full-duplex, Coded-OFDM, SIC*

1. INTRODUCTION

Various methods exist to establish communication links between two nodes, such as utilizing a physical connection like a cable or employing wireless technologies such as electromagnetic, optical, or acoustic waveforms. Underwater environments specifically rely on acoustic waveforms as the most viable and adaptable means to transmit information effectively across both short and long distances. Present-day commercial underwater acoustic communication (UAC) systems face two primary challenges, namely multipath interference and Doppler effects, when attempting to achieve successful communication between users or nodes.

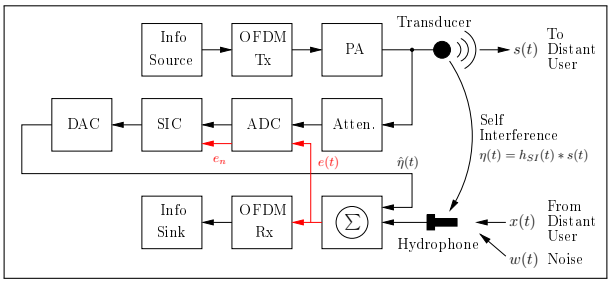

Figure 1. Proposed transceiver structure.

To address the interference caused by multipath, a technique called decision feedback equalizer (DFE) has been successfully employed in the past for single-carrier multichannel systems [1]. This approach utilizes timing and phase correction along with feedback to mitigate inter-symbol interference (ISI). By incorporating forward error correction (FEC) into the DFE framework, the system can exploit accurate decision feedback and employ iterative decoding, resulting in improved performance even at lower signal-to-noise ratio (SNR) levels [2].

Alternatively, multicarrier systems such as orthogonal frequency division multiplexing (OFDM) can combat ISI by transforming frequency-selective multipath into narrowband frequency non-selective channels [3]. This enables the use of a more efficient single-tap equalizer per subcarrier. OFDM is commonly combined with FEC to provide frequency diversity and enhance performance in

the presence of Doppler effects induced by movement [4].

In the past twenty years, there has been extensive research focused on underwater acoustic communication (UAC). However, due to the limited bandwidth of the UAC channel, the majority of the research has concentrated on the half-duplex (HD) mode of operation using time division duplexing (TDD). As a result, currently available commercial UAC systems are predominantly based on HD-TDD. This means that transmission and reception cannot occur simultaneously in terms of time or frequency. Recently, researchers have started exploring full-duplex (FD) systems [6], [7], but the inherent bandwidth constraints of the UAC channel make it impractical to achieve high data rate links using FD through frequency division multiplexing. Therefore, the only viable approach for implementing FD in UAC is by allowing overlapping transmissions in both frequency and time, and utilizing digital or analog cancellation techniques to address self-interference (SI) [6], [8].

This paper introduces a full-duplex underwater acoustic (FD-UAC) system that employs quasi-cyclic low-density parity check codes (QC-LDPC), quadrature phase shift keying (QPSK) modulation, and orthogonal frequency division multiplexing (OFDM) to mitigate the effects of noise and multipath interference. To address self-interference (SI), a novel method called successive interference cancellation (SIC) is proposed. This method utilizes the attenuated signal from the power amplifier's output to train the SIC filter weights. The system's performance is evaluated using experimental data collected during sea trials conducted in the North Sea off the coast of the UK.

2. SYSTEM MODEL

In this section, we present the system model, which includes the transmitter, the channel and receiver for the proposed FD-UAC C-OFDM system.

2.1 Transmitter

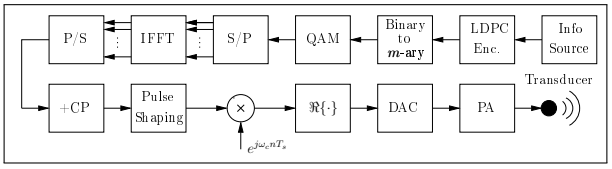

Figure 2. Proposed transmitter structure.

The generic block diagram of the transceiver structure for the proposed coded QC-LDPC OFDM FD system is shown in Fig. 1, while the transmitter part is illustrated in more detail in Fig. 2. The information to be transmitted is first encoded using a Quasi-cyclic LDPC (QC-LDPC) code and interleaved to protect against potential burst channel errors. Subsequently, the interleaved bits are grouped into pairs of 2 bits and mapped to a Gray-encoded quadrature phase shift keying (QPSK) constellation to improve spectral efficiency in the transmission. Following modulation, the QPSK symbols are grouped in blocks of dimension N and an inverse fast Fourier transform (IFFT) is applied to the block to transfer the signal into to time domain, where a cyclic prefix is appended to protect the OFDM symbol samples from inter-block interference (IBI). The cyclic prefix (CP) length is typically selected to be longer than the expected multipath delay spread of the channel. Finally, the OFDM symbol samples are pulse-shaped and frequency up-converted to a carrier frequency of f_c to exploit the transducer resonance and improve its transmission efficiency. The OFDM waveform is then amplified by an audio power amplifier that drives the transducer. The transmit power is adjusted so that the required signal-to-noise ratio (SNR) is satisfied to achieve the expected bit error rate (BER) at the distant node.

2.2 FD-UAC Channel Model

Assuming shallow-water type of FD-UAC channel, the received signal is given an

$$r(t) = x(t) + \eta(t) + v(t), \tag{1}$$

where $x(t)$ is the received signal from the distant node, i.e.

$$x(t) = h_d(\tau; t) * s_d(t), \tag{2}$$

with $h_d(\tau; t)$ and $s_d(t)$ being the underlying channel impulse response (CIR) and transmitted signal of the distant node, respectively. Furthermore, $\eta(t)$ is the SI from the local transmission given as

$$\eta(t) = h_{SI}(\tau; t) * s(t), \tag{3}$$

where $h_{SI}(\tau; t)$ and $s(t)$ are the local SI CIR and transmitted signal, respectively. Finally, $v(t)$ denotes the additive ambient noise present in the water column. It is worth noting that the variable τ is the multipath delay spread and the operator $*$ denotes the linear convolution operation.

Both the local and distant node CIRs can be modelled using a linear tapped-delay line filter model with finite set of time-varying coefficients. However, the delay spread of the SI is significantly longer than that of the CIR of the distant node and typically spans several seconds, while the distant CIR is much shorter typically in the ms range.

In [6], it was demonstrated that the envelope of the SI-CIR, $h_{SI}(\tau)$ can be empirically approximated as

$$|h_{SI}(\tau)| = \frac{0.15}{1 + \frac{\tau}{0.04\ \mathrm{s}}} \tag{4}$$

This is demonstrated in Fig. 3, where the envelope of the SI-CIR envelope is shown using red lines.

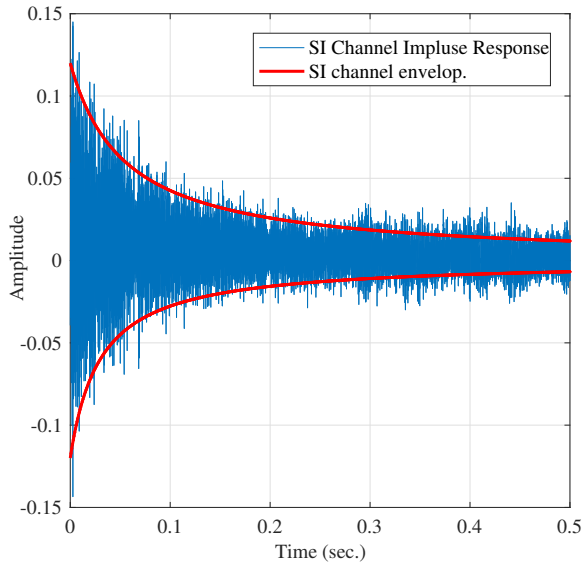

Figure 3. SI CIR and envelope for a typical shallow-water channel with depth 48 m.

2.3 Receiver

The SIC structure employed in the system is a finite impulse response (FIR) filter with a length of L, chosen to encompass significant portion of SI. The optimization of filter coefficients, denoted as $\mathbf{w}_n$, is achieved by minimizing a cost function. When using a least mean squares (LMS) algorithm, the cost function corresponds to the average mean squared error (MSE), represented as $J_n = E\{|e_n|^2\}$ [9]. Alternatively, if the normalized LMS (NLMS) algorithm is utilized for optimizing the SIC filter weights, the cost function $J_n = ||\mathbf{w}_{n+1} - \mathbf{w}_n||^2$ is minimized subject to the constraint $\mathbf{w}_{n+1}^H \mathbf{u}_n = d_n$, where d_n represents the desired signal and u_n represents the FIR filter memory [10]. The NLMS algorithm is a type of constrained optimization algorithm that seeks to minimize the norm of the difference between successive filter weights.

These algorithms exhibit low computational complexity suitable for practical implementation, although they may suffer from slow convergence [10]. For scenarios where higher computational complexity is permissible, a fast implementation of the recursive least squares (RLS) algorithm can be employed. In this case, the cost function becomes a weighted sum of the past N errors, i.e., $J_n = \sum_{i=0}^{n} \lambda^{n-i} |d_i - \mathbf{w}_n^H \mathbf{u}_i|^2$ [10]. However, when the size of the SIC filter exceeds 100 ($L > 100$), the computational complexity of RLS becomes impractical. As an alternative, the fast RLS version, as introduced in [11], can be utilized. This version takes advantage of the fact that only one sample in the filter memory changes per iteration, resulting in a computationally attractive solution for hardware implementations. The fast RLS algorithm entails a total computational complexity of $7L + 14$ operations per iteration and 2 divisions [11]. For a more detailed understanding of the equations required for implementation, the original paper by Cioffi & Kailath is recommended for reference [11].

To optimize the coefficients of the adaptive successive interference cancellation (SIC) filter, an initial training phase is conducted using a binary phase shift keying (BPSK) modulated pseudo-noise (PN) code. The PN code is chosen to possess a favourable autocorrelation sequence. Typically, an m-sequence is employed, with its length selected to be at least as long as the anticipated local multipath delay spread that induces self-interference (SI). It is worth noting that there is no advantage in using higher order modulations during training. Furthermore, the PN chips are multiplied with $(1 + j)$ to fit within the QPSK constellation and avoid a phase jump during the transition from training to data transmission.

As the PN code is known, the transceiver iteratively adjusts the coefficients of the adaptive SIC filter until the MSE between the known BPSK modulated PN code and the received SI signal is minimized. It is important that the training is performed at the start of the transceiver operation in the absence of a signal transmitted from the distant node with similar modulation characteristics. This is required in order to prevent the SIC filter attempting to cancel the distant signal and to speed-up convergence. Prior

to digitization by an analog-to-digital converter (ADC), the MSE is computed using an analog difference amplifier, which functions as a voltage subtractor. This is done to prevent saturation of the ADC caused by the SI signal. To perform this task, a low-noise, low-distortion, high-bandwidth operational amplifier capable of rail-to-rail operation is necessary. An example of such an amplifier is the LT1630, which operates with a supply voltage range (> 12 V) significantly larger than the dynamic range of the ADC (< 5 V).

It is important to note that the error signal is tapped before the digital bandpass filter, as indicated in Fig. 1. The adaptive SIC filter is trained during the duration of the PN code, and the obtained coefficients are stored at the end of the training phase for subsequent utilization and further adaptation in the FD mode. The NLMS algorithm is employed to optimize the coefficients, with the filter size chosen to cover up to 25% of the local SI.

3. EXPERIMENTAL RESULTS

This section presents the experimental outcomes obtained from seatrials conducted in the North Sea, UK. The geographical location off the coast of Tynemouth is depicted in Fig. 4, while Fig. 5 illustrates the specific FD-UAC scenario. Additionally, Fig. 6 showcases the measurement set-up employed during the trials. For the BER results presented in this paper, two scenarios for the distant node are considered, i.e. 500 m and 1 km, respectively.

The selected scenario reflects typical conditions found in shallow water channels, with a water column depth of $d_w = 48$ m. To deploy the Tx transducer and Rx hydrophone, the same line shown in Fig. 5 was used, with the Tx positioned at a depth of $d_{Tx} = 10$ m and the Rx positioned at a depth of $d_{Rx} = 5$ m. This configuration was chosen to ensure minimal interaction with the dynamic water surface. It is worth noting that exploiting the toroidal characteristics of the transducer in the z-axis helps to mitigate SI.

During the sea experiments, the signals were recorded using a Zoom F4 audio recorder featuring a 24-bit analog-to-digital converter (ADC) with a sampling frequency of $f_s = 48$ kHz. To bring the signal strength from the output of the power amplifier (PA) within line level range (1V rms), a passive attenuator was employed to record the signal after being amplified by the PA.

The noise spectra observed in the measured underwater acoustic channel are depicted in Fig. 7 and 8, both before and after undergoing bandpass filtering, respectively.

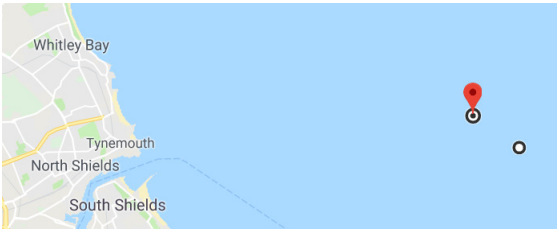

Figure 4. Location: Co-ordinates: (start) 55 00.981,-01 13.185 (stop) 55 01.534, -01 14.627.

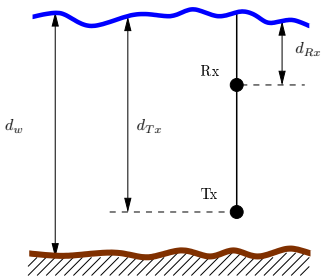

Figure 5. FDUAC scenario: hard bottom, $d_{Tx} = 10$ m, $d_{Rx} = 5$ m, $d_w = 48$ m.

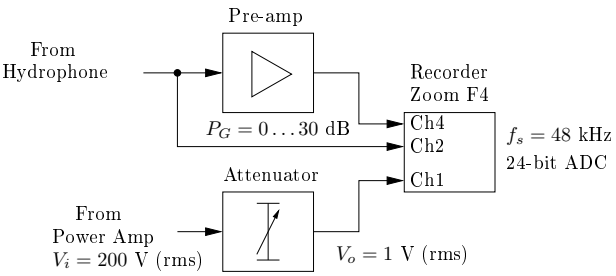

Figure 6. Measurement setup.

The frequency range covered extends from 0 up to half of the sampling frequency, which is 24 kHz. Upon closer examination of the figures, it becomes evident that the overall background level, set by the combination of in-band self-interference (SI) and ambient noise, rests at approximately -30 dB. The ambient noise encompasses a mixture of anthropogenic noise, including a tone at around 19 kHz, as well as natural background noise stemming from various sources like rain, wind, waves, and biolog-

Table 1. System parameters.

Parameter	Value
Carrier Frequency f_c (kHz)	12
Bandwidth B (kHz)	8
Number of Subcarriers	2048
Cyclic Prefix	64
Code Rate	1/2

ical activities such as fish sounds, marine mammal vocalizations, and snapping shrimp noise. Following the bandpass filtering process, the out-of-band interferences are effectively eliminated, leaving the signal ready for frequency downconversion and subsequent utilization as input for the SIC filter.

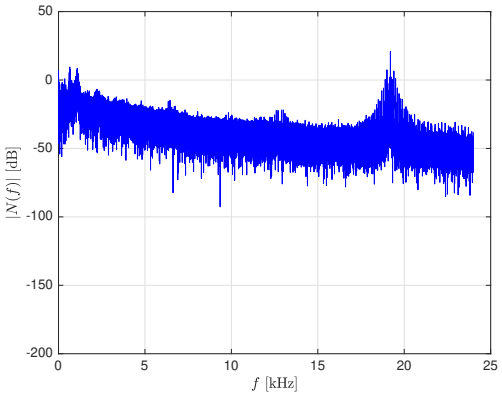

Figure 7. Noise of the raw received signal during silent period.

Fig. 9 and 10 depict the BER and Signal to Interference and Noise Ratio (SINR) over time (packet index) for two FD transmissions at distances of 1 km and 500 m, respectively. It is worth noting that the performance of the 1 km transmission achieves a lower BER due to the shorter multipath spread of the underlying CIRs. This is also evident from the higher SINR achieved for the 1 km transmission, which is shown in Fig. 10. It is worth noting that it was not possible to further improve the performance of the 500 m case by increasing the number SIC filter coefficients or by using RLS for faster adaption. The performance appears to be limited by the time-varying multipath characteristics between the distant node and the local transceiver rather than the residual SI after the SIC.

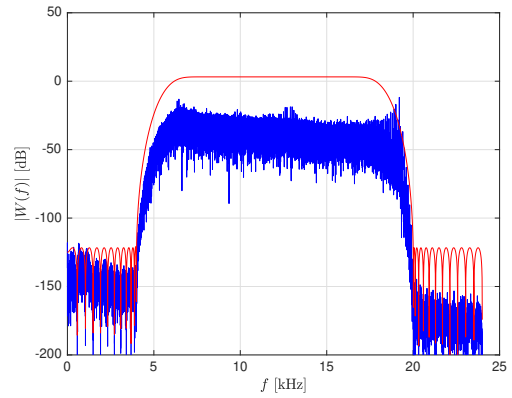

Figure 8. Noise of the filtered received signal during silent period.

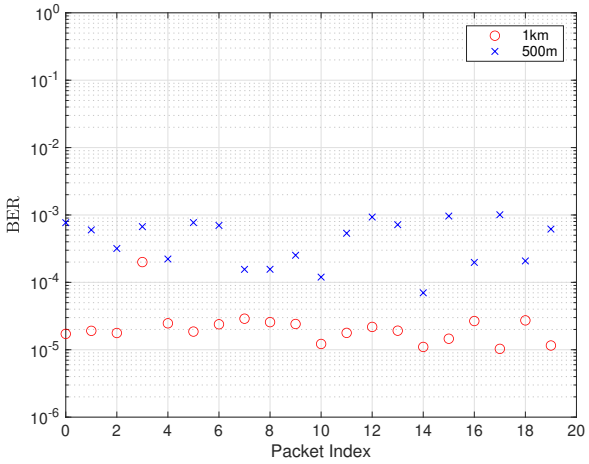

Figure 9. BER over time for 1 km and 500 m FD transmissions.

4. CONCLUSIONS

This paper introduced an FD-UAC system and its performance was evaluated using experimental signals obtained from sea trials conducted in the North Sea off the coast of the UK. The proposed system utilized QC-LDPC codes, QPSK modulation, and OFDM to overcome challenges posed by noise and multipath effects. To address self-interference (SI), a cancellation method was proposed, which involved tapping the attenuated signal from the power amplifier's output to train the weights of the SIC filter. The results demonstrated the effectiveness of the pro-

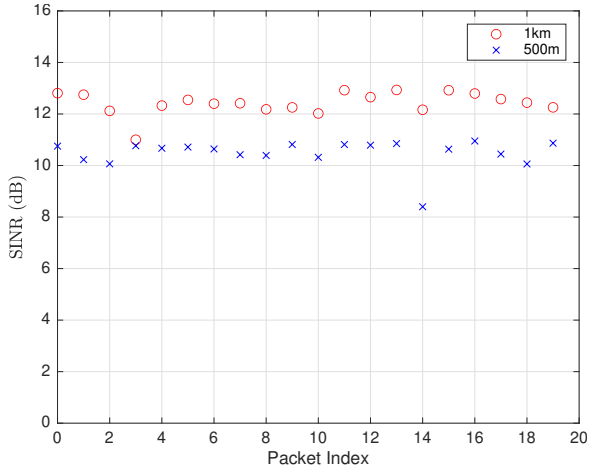

Figure 10. SINR over time for 1 km and 500 m FD transmissions.

posed transceiver by successfully decoding distant transmissions from a user located 1 km away. Future research will focus on implementing SIC using infinite impulse response (IIR) filters to reduce the complexity associated with the lengthy FIR filter implementation. Additionally, efforts will be directed towards developing fast algorithms for updating the filter weights of the IIR filters.

5. ACKNOWLEDGEMENTS

This work was supported by the EPSRC under project EP/R002665/1, Full-Duplex for Underwater Acoustic Communications. The authors would like to thank the Research Council for this funding.

6. REFERENCES

[1] M. Stojanovic, J. A. Catipovic and J. G. Proakis, "Phase-coherent digital communications for underwater acoustic channels," in *IEEE Journal of Oceanic Engineering,* vol. 19, no. 1, pp. 100-111, Jan. 1994.

[2] C. P. Shah, C. C. Tsimenidis, B. S. Sharif and J. A. Neasham, "Low-Complexity Iterative Receiver Structure for Time-Varying Frequency-Selective Shallow Underwater Acoustic Channels Using BICM-ID: Design and Experimental Results," in *IEEE Journal of Oceanic Engineering,* vol. 36, no. 3, pp. 406-421, July 2011.

[3] S. Zhou and Z. Wang, *OFDM for Underwater Acoustic Communications*, 1st. ed., (Wiley Publishing, 2014).

[4] A.E. Abdelkareem, B.S. Sharif and C.C. Tsimenidis, "Adaptive time varying doppler shift compensation algorithm for OFDM-based underwater acoustic communication systems," *Ad Hoc Networks,* vol. 45, pp. 104-119, 2016.

[5] S. Myung, K. Yang and J. Kim, "Quasi-cyclic LDPC codes for fast encoding," *IEEE Transactions on Information Theory*, vol. 51, no. 8, pp. 2894-2901, **(2005)**.

[6] B. A. Jebur, C. T. Healy, C. C. Tsimenidis, J. Neasham and J. Chambers, "In-Band Full-Duplex Interference for Underwater Acoustic Communication Systems," *IEEE OCEANS 2019* - Marseille, Marseille, France, 2019, pp. 1-6.

[7] C. Healy, B. Jebur, C. C. Tsimenidis, J. Neasham and J. Chambers, "Full-duplex channel analysis for underwater acoustic communications," *Underwater Acoustics Conference and Exhibition*, Crete, Greece, pp. 251-258, June 2019.

[8] L. Shen, B. Henson, Y. Zakharov and P. Mitchell, "Digital Self-Interference Cancellation for Full-Duplex Underwater Acoustic Systems," *IEEE Trans. on Circuits and Systems II: Express Briefs*, vol. 67, no. 1, pp. 192-196, Jan. 2020.

[9] J. G. Proakis et al, *Algorithms for Statistical Signal Processing*, Prentice Hall, 2002.

[10] S. Haykin, *Adaptive Filter Theory*, 4th Ed., Pearson, 2014.

[11] J. Cioffi and T. Kailath, "Fast, recursive-least-squares transversal filters for adaptive filtering," *IEEE Transactions on Acoustics, Speech, and Signal Processing*, vol. 32, no. 2, pp. 304-337, April 1984.